American Journal of Pathology, Vol. 149, No. 2, August 1996

Immunodetection of Histone Epitopes Correlates with Early Stages of Apoptosis in Activated Human Peripheral T Lymphocytes

Susan J. Zunino, Manoj K. Singh, Julia Bass, and Louis J. Picker

From the Laboratory of Molecular Pathology, Department of Pathology, The University of Texas Southwestern Medical Center, Dallas, Texas

By coupling intracellular staining with terminal deoxynucleotidyl transferase (TdT)-mediated labeling of internucleosomal DNA strand breaks in a flow cytometric assay, we observed a strong correlation between apoptosis-associated DNA strand breaks and immunoreactivity with the monoclonal antibody (MAb) B-F6 in activated human peripheral blood T lymphocytes (PBTs). Although MAb B-F6 has been reported to be specific for the cytokine interleukin-6, Western blot analysis of activated PBT lysates revealed that the predominant protein band detected by this MAb was 17 kd (p17), distinct from the 23-kd core protein and 26- to 30-kd mature glycosylated forms of interleukin-6. Immunoaffinity isolation and amino-terminal amino acid sequence analysis of p17 revealed identity with the histone H2B, a finding confirmed by Western blot analysis of purified histones and by similar staining of activated PBTs with an unrelated anti-histone MAb. Neither histone staining nor DNA strand breakage was observed in freshly isolated PBTs; however, after T cell activation, histone immunoreactivity appeared to precede the appearance of DNA strand breaks, with both increasing to a maximal level by day 3 after activation. Two-parameter confocal immunofluorescence microscopy of histone and DNA staining confirmed a lack of histone immunoreactivity in viable cells and demonstrated co-localization of histone epitopes with abnormally clumped chromatin in apoptotic cells. These data indicate that alteration of histone epitope accessibility is a marker of early apoptosis and suggest that multiparameter flow cytometric analysis of intracellular epitopes may be a powerful tool in the elucidation of intracellular mechanisms of apoptosis. (Am J Pathol 1996, 149:653–663)

The ability of T lymphocytes to undergo programmed cell death, or apoptosis, is critical to the overall regulation of the immune response. In the thymus, apoptosis plays a major role in thymocyte selection and thus directs the development of the T-lineage antigen receptor repertoire.[1] In the peripheral immune system, apoptosis regulates T cell responsiveness to antigen,[2,3] preventing uncontrolled clonal expansion and possibly molding the repertoire and function of the memory subset. Activation-induced apoptosis can be observed in immature thymocytes,[4] in transformed T cell lines,[5] and in peripheral blood T lymphocytes.[6] Stimuli that induce activation-dependent apoptosis in peripheral T cells include nonspecific mitogens, specific antigen triggering through the CD3 complex, ligation of the T cell receptor with specific antibody, and superantigens.[7–9] Apoptosis of activated peripheral T cells appears to be triggered by the expression and subsequent interaction of Fas (CD95) and its ligand,[3] resulting in a cascade of events that at present remain unclear.

A hallmark of apoptosis in T cells and other cell types is the oligonucleosomal fragmentation of the genome by activation of endogenous endonucleases.[10] The classical method for detecting endonuclease digestion of chromatin is through the visualization of the oligonucleosomal ladder by agarose gel electrophoresis.[11] Recently, a more sensitive method has been developed to analyze oligonucleo-

Supported by National Institutes of Health grant AI31545 and an award of the President's Research Council of the University of Texas Southwestern Medical Center. M. Singh was supported by a fellowship grant from the World Health Organization.

Accepted for publication March 29, 1996.

Address reprint requests to Dr. Louis J. Picker, Department of Pathology, The University of Texas Southwestern Medical Center, 5323 Harry Hines Blvd., Dallas, TX 75235-9072.

somal fragmentation in apoptotic cells using terminal deoxynucleotidyl transferase to end-label DNA strand breaks (the TdT strand break assay).[12] Here, we adapted this assay to multiparameter flow cytometry to simultaneously examine DNA strand breaks, cell surface protein expression, and accumulation of intracellular proteins in activated human peripheral blood T cells (PBTs). During a preliminary study of apoptosis and intracellular cytokine expression in activated peripheral T cells, we discovered a correlation between DNA strand breaks and the binding of the anti-interleukin (IL)-6 monoclonal antibody (MAb) B-F6. Characterization of the binding of MAb B-F6 indicated that a 17-kd protein (p17) was responsible for the correlation we observed with apoptotic PBTs. By immunoaffinity purification and subsequent amino acid sequencing, we determined that p17 was histone H2B.

Accumulation of large amounts of histones has been observed in T cells infected with human immunodeficiency virus (HIV) by day 3 after infection.[13] In this study, crude protein lysates of cells analyzed by sodium dodecyl sulfate polyacrylamide gel electrophoresis (SDS-PAGE) gels showed increasing levels of extrachromosomal histones, which was proposed to be due to oligonucleosomal fragmentation of the chromatin. We report here that flow cytometric immunodetection of histone H2B not only correlates with apoptosis in activated human peripheral T cells but also appears to be an early marker of this process, preceding TdT detection of DNA strand breaks. Moreover, the techniques presented in this study provide a sensitive and convenient method by which to monitor the progressive changes in chromatin structure that occur during apoptosis.

Materials and Methods

Preparation of Purified T Lymphocytes and Cell Culture

Human mononuclear cells from normal adult peripheral blood (PBMCs) were isolated by density gradient centrifugation over Ficoll-Hypaque (Histopaque 1077, Sigma Chemical Co., St. Louis, MO). For most analyses, T lymphocytes (>95% $CD3^+$) were purified from PBMCs by using human T cell enrichment columns (R&D Systems, Minneapolis, MN). Purified T lymphocytes were cultured in RPMI 1640 (GIBCO BRL, Gaithersburg, MD) supplemented with 10% heat-inactivated fetal bovine serum (GIBCO BRL), 2 mmol/L L-glutamine (Sigma), 10 mmol/L hepes (Sigma), 5×10^{-5} 2-mercaptoethanol (Sigma), 1 mmol/L sodium pyruvate (Sigma), and 10 U/ml penicillin G/10 mg/ml streptomycin (GIBCO BRL). T cells were stimulated with 20 ng/ml phorbol myristate (PMA; Sigma) plus 0.75 μg/ml ionomycin (Sigma) or 1 μg/ml phytohemagglutinin (Wellcome Diagnostics, Greenville, NC) for the times indicated in the text. In some experiments, T cells were activated through the T cell receptor by adding PBTs to six-well plates that had been coated with 10 μg/ml anti-CD3 antibody at 4°C overnight. The Jurkat T cell line was obtained from L. Davis at University of Texas Southwestern Medical Center and was maintained in culture in the RPMI medium described above.

For freshly isolated PBMCs, small quantities of donor blood were obtained and promptly centrifuged in Vacutainer cell preparation tubes (Becton Dickinson Vacutainer Systems, Franklin Lakes, NJ). After collection of the PBMC fraction, the cells were immediately processed as described for intracellular staining.

Antibodies

Fluorescein isothiocyanate (FITC)-conjugated mouse anti-human Leu 3a (CD4), Leu 2a (CD8), and Leu 4 (CD3) MAbs and phycoerythrin (PE)-conjugated streptavidin were obtained from Becton Dickinson Immunocytometry Systems (San Jose, CA). The non-neutralizing anti-human IL-6 MAb clone B-F6, the neutralizing anti-human IL-6 clone B-E8, and anti-human IL-2 MAb clone B-G5 were obtained from Biosource International (Camarillo, CA). An additional anti-human IL-6 MAb (1618–01) was purchased from Genzyme (Cambridge, MA), and a rabbit polyclonal anti-human IL-6 IgG preparation (batch 91–100) was obtained from Intracel (Cambridge, MA). The pan-anti-histone MAb clone H11–4 was purchased from Boehringer Mannheim (Indianapolis, IN), and a control mouse IgG1 MAb was purchased from Sigma. Second-stage reagents used in this study included a Tri-color (PE-Cy5 tandem reagent)-conjugated goat anti-mouse IgG1 from Caltag Laboratories (So. San Francisco, CA) and a FITC-conjugated anti-mouse IgG from TAGO (Burlingame, CA).

Intracellular Staining

Purified T cells were stained for intracellular cytokines as described[14,15] with modifications. Brefeldin A (Sigma; 10 μg/ml) was routinely added to the PBT culture 4 hours before harvesting for kinetics analyses to allow intracellular accumulation of secreted proteins. PBTs were then fixed and permeabilized for

10 to 15 minutes with 4% paraformaldehyde (Sigma), 0.1% saponin (Sigma) in Hank's balanced salt solution containing 10 mmol/L Hepes buffer (pH 7.2). After washing twice, the cells were incubated with the anti-cytokine MAb for 30 minutes on ice at concentrations of 10 μg/ml for control IgG1, clone B-F6, and clone H11–4 and 25 μg/ml for clone B-G5. The cells were washed once and incubated with appropriately titrated Tri-Color or FITC-conjugated secondary antibody for 30 minutes on ice.

Assays for Apoptosis

Apoptosis was detected in T cells by two methods. After intracellular staining with the anti-cytokine antibodies, the apoptotic population was detected using the TdT-mediated DNA strand break detection assay[12] with some modifications. Briefly, the purified T cells were refixed after the intracellular staining and washed, and then the reaction mixture containing 10 U of TDT (Boehringer Mannheim), 0.1 mmol/L dithiothreitol (GIBCO BRL), and 0.5 nmol/L biotinylated dCTP (GIBCO BRL), 1X buffer (Boehringer Mannheim), and 1 mmol/L $CoCl_2$ was added to the cell pellet. Control tubes contained reaction mixture without the enzyme. The cells were incubated for 30 minutes at 37°C, washed, and then incubated with PE-conjugated streptavidin for 30 minutes on ice. After washing, the cells were resuspended in 1% paraformaldehyde before flow cytometric analysis.

The second method, based on the differential uptake of the dyes 7-aminoactinomycin D (7-AAD) and Hoechst 33342,[16] was used to sort apoptotic *versus* viable cell populations of activated PBTs. Briefly, 10^6 activated T cells were incubated for 7 minutes at 37°C in 1 ml of phosphate-buffered saline (PBS) containing 1% bovine serum albumin plus 1 μg/ml Hoechst 33342 (Molecular Probes, Eugene OR). Cells were immediately placed on ice, and 7-AAD (Molecular Probes) was added at a final concentration of 1 μg/ml. The cells were incubated on ice for 10 minutes and were immediately analyzed or sorted into apoptotic and viable cell populations on the FACStar Plus flow cytometer (Becton Dickinson). Sorted cells were collected and lysed as described below for Western blot analysis.

Flow Cytometry and Immunofluorescence Analysis

Five-parameter immunofluorescent analysis was performed on a FACScan or a FACSort flow cytometer (Becton Dickinson) using FITC, PE, and Tri-Color (PE-Cy5 tandem) as the three fluorescent parameters. Fluorescence-activated cell sorting (FACS) of viable *versus* apoptotic T cell populations was performed on a dual-laser (ultraviolet and 488-nm beams) FACStar Plus flow cytometer. Multiparameter data files were analyzed with the PAINT-A-GATE^{Plus} software (Becton Dickinson). All analyses were performed using appropriate scatter gates to exclude cellular debris and aggregated cells. Freshly isolated PBMCs were surface stained with anti-CD3 antibody for identification and gating on PBTs.

Preparation of Protein Lysates and Western Blot

Fresh tonsil tissue was obtained through the tissue acquisition service within the Department of Pathology at the University of Texas Southwestern Medical Center. Samples of tonsil were minced and filtered through nylon mesh to remove debris before lysing. For Western blot analysis and protein purification, lysates of tonsil cells or activated (2 to 3 days of PMA plus ionomycin) PBTs were made by vortexing 5×10^7 cells/ml lysis buffer containing 1% Nonidet P-40 (Sigma), 50 mmol/L Tris-Cl, pH 8, 150 mmol/L NaCl, and the following proteinase inhibitors (Boehringer Mannheim): 1 μg/ml aprotinin, 10 μg/ml chymostatin, 10 μg/ml E64, 0.5 mg/ml EDTA, 2 μg/ml leupeptin, 100 μg/ml Pefabloc SC, and 2 μg/ml pepstatin. Lysates were electrophoresed on 15% SDS-polyacrylamide reducing gels and electroblotted on to nitrocellulose.[17] For blots requiring the use of multiple antibodies for staining, the membranes were placed in a Miniblotter 25 (Immunetics, Cambridge, MA). Recombinant IL-6 protein was purchased from Genzyme Corp. (Cambridge, MA) and provided a positive control for staining with MAb B-F6. For Western blots of histone proteins, calf thymus histones H1, H2A, H2B, H3, and H4 (Boehringer Mannheim) were run in individual lanes on 15% reducing SDS-PAGE gels. Ponceau S (Sigma) was used to ensure the presence of protein before staining with control IgG1 or MAb B-F6. The ECL Western blotting system (Amersham Life Science, Arlington Heights, IL) was used for visualization of immunoreactive bands at vendor-suggested concentrations.

Immunoaffinity Protein Purification and Sequencing Analysis

Protein purification was performed by immunoaffinity chromatography. Approximately 1 mg of MAb clone

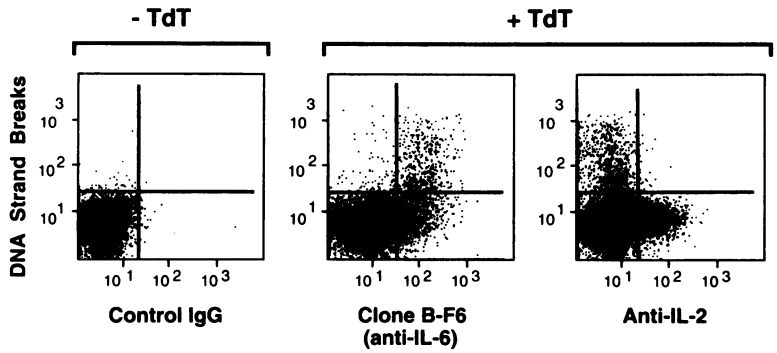

Figure 1. *B-F6-positive PBTs include a large population of apoptotic cells that is not observed with an anti-IL-2 antibody. Purified PBTs were activated with PMA plus ionomycin for 40 hours, and 10 μg/ml Brefeldin A was added to the cultures 4 hours before staining. Cells were stained intracellularly with control IgG1, MAb B-F6, or the anti-IL-2 MAb B-G5 followed by Tri-color-conjugated secondary antibody. DNA strand breaks were then end-labeled with biotinylated nucleotide by TdT, and these labeled strand breaks were visualized with PE-streptavidin. The profiles shown represent approximately 13,000 T cells, gated on light scatter signals to exclude debris and cell aggregates. The control profile shows the typical background staining observed when the TdT assay (with PE-streptavidin staining) is performed with the TdT enzyme omitted (negative control for the TdT assay) and when an irrelevant isotype-matched MAb is substituted for the BF-6 or B-G5 MAbs.*

B-F6 was bound to 1 ml of protein-G-Sepharose beads (Sigma) and chemically coupled with dimethylpimelimidate[17] (Sigma). Tonsil lysates were passed over the column, and protein was eluted with 0.1 mmol/L glycine, pH 2.5. Eluted fractions were analyzed for p17 by Western blotting. Fractions containing the protein were pooled and TCA precipitated.

Sequence analysis was performed as described.[18] The concentrated protein was electrophoresed, and the p17 band was located by Coomassie blue staining. Approximately 2 μg of protein was electroblotted to Immobilon-SQ paper (Millipore Corp., Bedford, MA). The amino-terminal amino acid sequence was acquired by Edman degradation on a Model 477A sequencer from Applied Biosystems (Foster City, CA). Analysis of the amino acids was performed on a model 420A amino acid analyzer (Applied Biosystems). The partial amino acid sequence was compared with proteins in the Intelligenetics Database.

Microscopic Analysis of Apoptotic Cells

Activated PBTs were stained as described above for intracellular proteins with 10 μg/ml control IgG1, clone B-F6, or clone H11–4. FITC-conjugated goat anti-mouse IgG was used as the secondary antibody. Cells were then treated for 15 minutes with RNAse (Sigma) at a concentration of 1 mg/ml, and 10 μg/ml propidium iodide in PBS was then added.[19] Cells were kept in the dark until analysis. Images were collected on a MRC600 LSCM confocal scanning unit (Bio-Rad, Microscience Division, Cambridge, MA) equipped with a krypton-argon laser (Ion Laser Technology, Salt Lake City, UT) and a Nikon Optiphot II microscope. Images were prepared from collected files using the Macintosh-based freeware NIH Image v1.58.

Results

Correlation between Apoptosis and B-F6 Staining

During an initial examination of the intracellular production of different cytokines in activated T lymphocytes by flow cytometry, we observed that the population of T cells staining with the anti-IL-6 MAb clone B-F6 were predominantly clustered within the light-scatter region consistent with small, condensed, apoptotic cells. As oligonucleosomal DNA fragmentation is a hallmark of apoptosis, we incorporated the TdT assay[12] into our staining protocol to confirm that the B-F6-positive activated PBTs were undergoing apoptosis. After staining the cells with anti-cytokine antibodies, we then end-labeled DNA strand breaks with biotinylated nucleotides and fluorochrome-conjugated streptavidin. Our results indicated that the activated PBTs staining positive with clone B-F6 included a large population of cells undergoing apoptosis (Figure 1). Note that negative control cells stained with an irrelevant mouse IgG1 and treated with the TdT reaction mix without the TdT enzyme and then stained with the streptavidin-PE displayed no significant staining. The correlation between B-F6 staining and apoptosis was not observed with the anti-IL-2 clone (Figure 1) or other anti-cytokine antibodies examined (data not shown). PBTs that were stimulated with PMA plus ionomycin, phytohemagglutinin, or anti-CD3 antibody all showed a similar

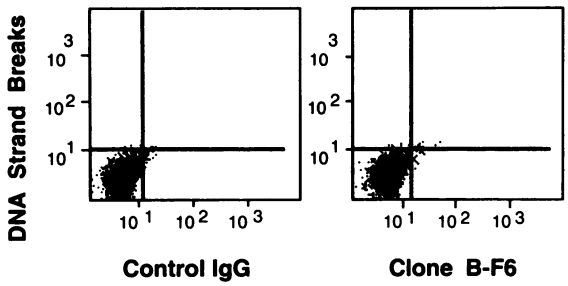

Figure 2. *Freshly isolated PBTs lack immunoreactivity with B-F6 and DNA strand breaks. PBMCs were immediately and rapidly isolated from blood and then simultaneously assessed for B-F6 reactivity, DNA strand breaks using the TdT labeling technique, and CD3 expression to identify T cells. The profiles shown represent approximately 4000 T cells (gated on CD3$^+$ and on light-scatter parameters to exclude debris and aggregates).*

correlation between apoptosis and staining with clone B-F6. This correlative pattern of staining was identified in both the CD4$^+$ and CD8$^+$ T cell subsets (data not shown). As will be addressed in more detail below, the delineation of apoptotic T cells was unique to the B-F6 clone; two distinct anti-IL-6 MAbs were essentially nonreactive with activated PBTs when examined in parallel (data not shown).

Kinetics of Apoptosis in T Cells

We found that the usual processing time and the mechanical manipulations required to produce purified T cells appeared to damage a subset of the cells and resulted in a background pattern of staining for both B-F6 staining and DNA strand breaks (particularly the latter) if these stains were immediately performed (not shown). To reduce the presence of this activation-independent cell damage and determine whether normal, unstimulated (fresh) circulating T cells truly stained positively for B-F6 and/or DNA strand breaks, PBMCs were isolated rapidly from whole blood and immediately fixed. Intracellular staining with clone B-F6 (*versus* IgG1 control) and CD3, followed by the TdT strand break assay, was then performed. Figure 2 shows that the T cell component of freshly isolated PBMCs, identified by CD3 reactivity, had no detectable DNA strand breakage or B-F6 reactivity.

Kinetics analysis of activation-induced apoptosis in PBTs (Figure 3) showed that the strong correlation between B-F6 reactivity and apoptotic (DNA-strand-break-positive) cells was apparent by 18 hours after activation with PMA plus ionomycin and continued throughout the 88-hour time course. At early time points (eg, 4 hours), a small number of B-F6$^-$/strand-break-positive cells were observed (again, likely the result of cells directly damaged during the T cell purification procedure), but more importantly, at these early time points, a significant population of B-F6$^+$/strand-break-negative cells was present in the absence of B-F6$^+$/strand-break-positive cells. The presence of B-F6$^+$/strand-break-negative cells continued after the appearance of B-F6$^+$/strand-break-positive cells. Collectively, these data strongly suggest that B-F6 reactivity precedes the appearance of detectable DNA strand breaks during activation-induced T cell apoptosis and that there is continuous recruitment of T cell blasts into the apoptotic pathway.

Detection of a 17-kd Protein in Apoptotic PBTs

To characterize the B-F6 reactive protein in apoptotic cells, activated PBTs or spent cultures of the Jurkat T cell line were sorted into apoptotic and viable cell populations by FACS according to the differential uptake of two dyes, Hoechst 33342 and 7-AAD.[16] In this staining protocol, viable cells show low uptake of Hoechst 33342 and are impermeable to the vital dye 7-AAD. Cells in the early stages of apoptosis show increased uptake of Hoechst 33342 but remain impermeable to the 7-AAD dye, whereas in later stages of apoptosis the cell membrane loses

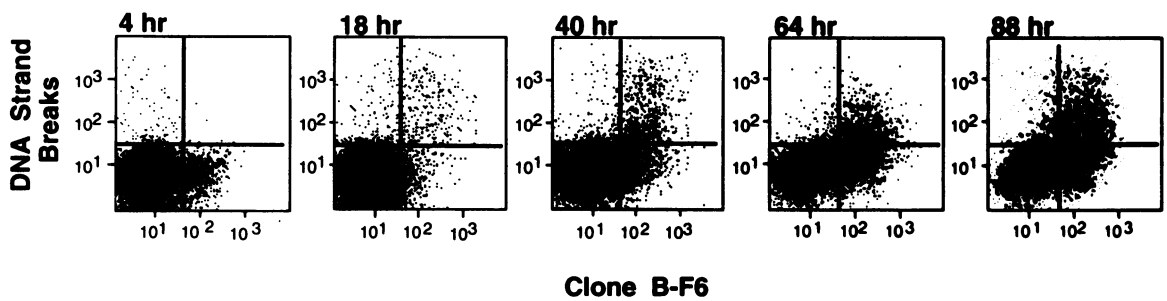

Figure 3. *B-F6 immunoreactivity appears to precede detection of DNA strand breaks during the evolution of activation-induced PBT apoptosis. Purified PBTs were activated with PMA plus ionomycin for the times indicated and then simultaneously assessed for B-F6 reactivity and DNA strand breaks using the TdT labeling technique (as performed in Figure 1). The profiles shown represent approximately 13,000 cells, gated on light-scatter parameters to exclude debris and aggregates.*

the ability to exclude 7-AAD and the cells become Hoechst 33342^{high} and 7-AAD^{+}. Figure 4A shows the typical sorting scheme used to isolate the apoptotic and viable cell populations. Figure 4, B and C, shows that a protein band of approximately 17 kd (p17) was preferentially detected with the B-F6 MAb in the apoptotic populations of both activated PBTs and Jurkat cells. Although some p17 was detectable in Hoechst 33342^{low}/7-AAD^{-} PBTs and Jurkat populations, p17 immunoreactivity in these viable cells was always considerably less than in the clearly apoptotic populations. Note in this figure that, whereas MAb B-F6 does react with recombinant IL-6 protein, this cytokine is 5 to 6 kd greater than p17. Specific B-F6-reactive or polyclonal anti-IL-6-reactive bands with a molecular weight consistent with *bona fide* IL-6 were either absent or very faint in these cell lysates. This finding, along with our aforementioned failure to flow cytometrically detect immunoreactivity with two distinct anti-IL-6 MAbs in activated PBTs, suggests that the BF-6 reactivity observed in apoptotic T cells by flow cytometry is predominantly, if not entirely, due to detection of p17.

Identity of p17

Preliminary studies of human tonsils revealed that this tissue was an abundant source of p17. Therefore, we isolated p17 from tonsil lysates by immunoaffinity chromatography with B-F6-coupled Sepharose beads. Figure 5A shows the 17-kd band that was isolated from the tonsil cells (lanes 2 and 3) migrated in SDS-PAGE at the same molecular weight as the p17 observed in PBT lysates (lane 1). After additional purification of affinity-isolated p17 by SDS-PAGE, amino-terminal amino acid sequencing was performed. Comparison of the resultant sequence with the protein database (Figure 5B) revealed p17 to be identical to histone H2B. Interestingly, alignment of the amino acid sequences for histone H2B and IL-6 revealed five amino acids that were identical within a 20-amino-acid region (Figure 5C).

Western blot analysis was utilized to confirm the cross-reactivity of clone B-F6 with histone H2B. Histones H1, H2A, H2B, H3, and H4 from calf thymus were blotted onto nitrocellulose and stained with clone B-F6 (Figure 6). As shown in Figure 6, the B-F6 MAb was highly cross-reactive with histone H2B (perhaps due to the limited amino acid homology described above), and this histone co-migrated on SDS-PAGE with the B-F6-defined p17 from activated PBT lysate.

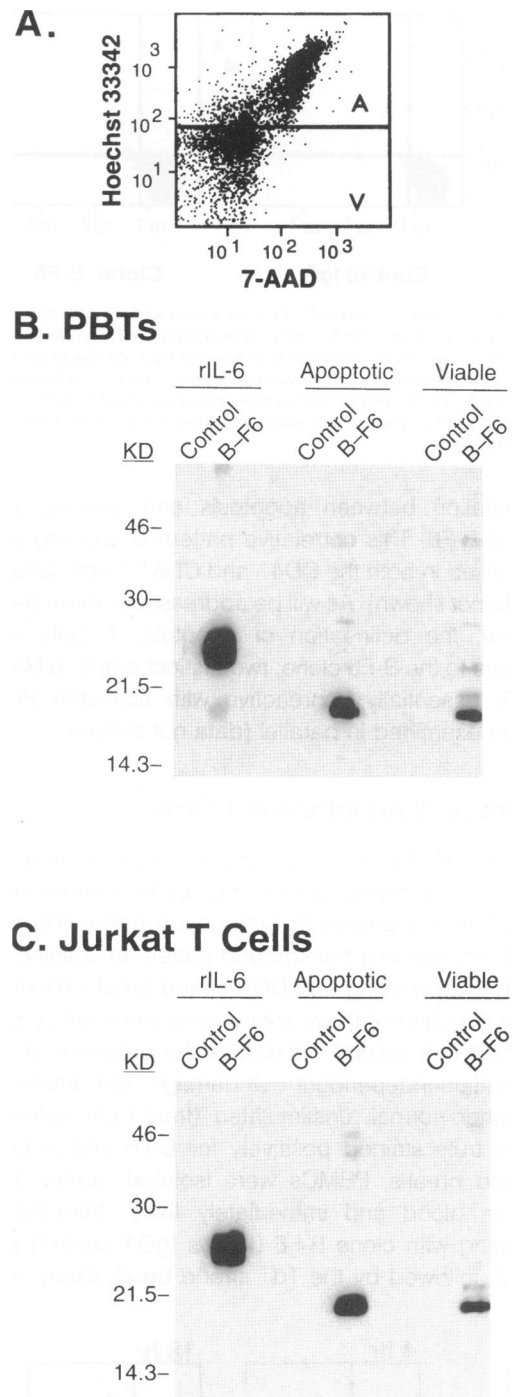

Figure 4. *B-F6 reacts with a 17-kd protein (p17) that is preferentially present in lysates of apoptotic PBTs and Jurkat T cells. PBTs were activated in culture with PMA and ionomycin for 40 hours. Jurkat T cells were allowed to grow in culture for 5 days without addition of fresh medium.* **A:** *Cells were then sorted into apoptotic (A) and viable (V) cell populations using the typical staining pattern as shown for uptake of Hoechst 33342 and 7-AAD. Sorted cells were collected and lysed for Western blot analysis at a concentration of* 5×10^7 *cells/ml lysis buffer, and equivalent amounts of lysate were electrophoresed on 15% SDS-PAGE gels. Recombinant IL-6 was also run on the gels as a positive control. After transfer to nitrocellulose, the blots were placed into a Miniblotter 25 apparatus and 50 μg/ml control IgG1 and MAb B-F6 were applied to individual lanes as indicated. Visualization of staining was achieved using the Amersham chemiluminescence kit.* **B:** *Apoptotic and viable PBTs.* **C:** *Apoptotic and viable Jurkat T cells.*

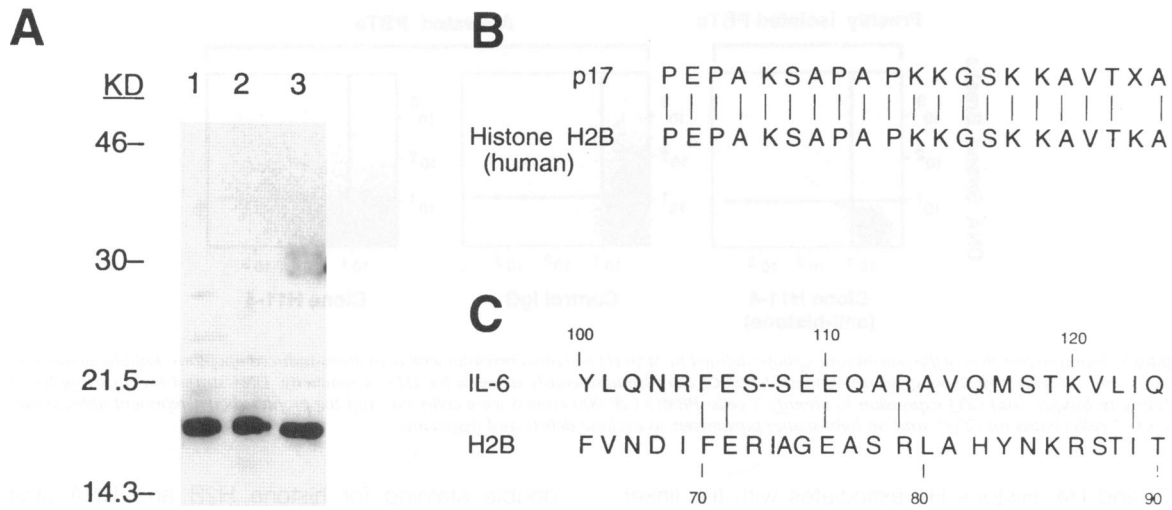

Figure 5. *The amino-terminal amino acid sequence of purified p17 is identical to histone H2B. Tonsil cell lysates were made at a concentration of* 5×10^7 *cells/ml lysis buffer and passed over a column containing MAb B-F6 chemically coupled to protein-G-Sepharose. Fractions were eluted with 0.1 mmol/L glycine, pH 2.5, and analyzed for the presence of p17 by Western blot. The appropriate fractions were pooled and TCA precipitated, and then p17 was futher purified by SDS-PAGE before amino-terminal amino acid sequencing.* **A:** *Activated PBT lysate* (**lane 1**), *tonsil lysate* (**lane 2**), *and affinity-purified p17* (**lane 3**) *were electrophoresed on 15% SDS-PAGE gels, blotted, and stained with MAb B-F6 to indicate that the 17-kd band migrates at a similar molecular weight in all three preparations.* **B:** *The amino-terminal amino acid sequence of p17 was compared with protein sequences using the Intelligenetics database software and was determined to be identical to the amino terminus of histone H2B.* **C:** *Histone H2B and IL-6 protein sequences were aligned to determine possible common epitopes by using the GCG Wisconsin database software.*

Detection of Histone Protein in Apoptotic PBTs

To further demonstrate that immunodetection of histone epitopes correlates with the onset of apoptosis, intracellular staining with a distinct pan-anti-histone MAb H11–4 was assessed in conjunction with DNA strand break analysis. As shown in Figure 7, unstimulated PBTs do not stain for either the H11–4-defined histone proteins or DNA strand breaks. However, activated PBTs demonstrated a similar correlation between DNA stand breaks and H11–4 immunoreactivity as was previously observed with clone B-F6.

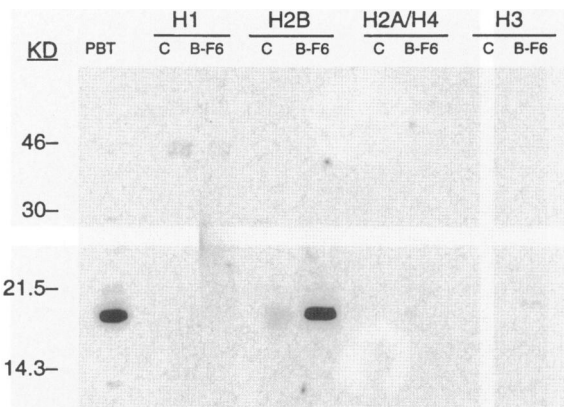

Figure 6. *Antibody B-F6 shows strong cross-reactivity with histone H2B but not other histone proteins. Calf thymus histones H1, H2A, H2B, H3, and H4 were electrophoresed on 15% SDS-PAGE gels, blotted, and stained with control IgG1 or MAb B-F6. BF-6 reactivity with activated PBT lysate was included for comparative purposes. Note the co-migration of p17 and histone H2B in the SDS-PAGE gels. Ponceau S staining was performed before staining with antibody to ensure the presence of the histone proteins on the blots.*

Cellular Localization of Protein

To determine the distribution of histone proteins with respect to the DNA in apoptotic cells, activated PBTs were stained intracellularly with either clone B-F6 or clone H11–4 followed by the addition of the DNA intercalating dye propidium iodide. As represented in Figure 8, non-apoptotic PBTs, identified by their diffuse pattern of DNA staining, did not show appreciable amounts of staining with either clone B-F6 or clone H11–4. In contrast, apoptotic cells, identified by their characteristic chromatin clumping and margination along the nuclear membrane or nuclear condensation and blebbing, stained positively with both clone B-F6 and H11–4. The positive staining for histone proteins with either antibody typically co-localized with the characteristically clumped chromatin in the apoptotic cells.

Discussion

Histone proteins are integral components of chromatin structure that serve to organize nuclear DNA into nucleosomal subunits.[20] Each nucleosome consists of DNA wrapped around a core histone octamer containing two molecules each of histone H2A, H2B,

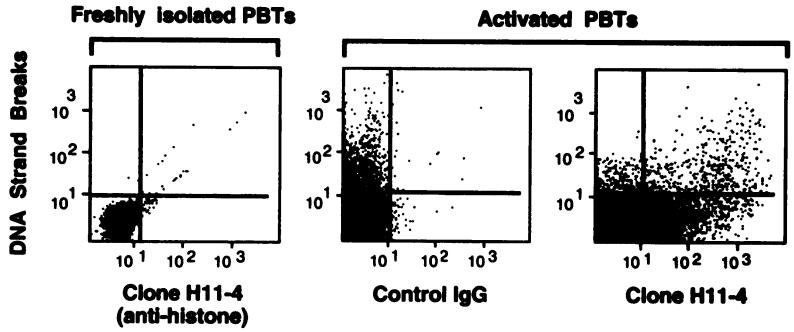

Figure 7. *Immunodetection of the pan-histone epitope defined by MAb H11–4 also correlates with activation-induced apoptosis. Rapidly isolated fresh PBMCs and 40-hour phytohemagglutinin-activated PBMCs were simultaneously assessed for H11–4 reactivity, DNA strand breaks using the TdT labeling technique, and CD3 expression to identify T cells. PBMCs (20,000 events) were collected, and the profiles shown represent approximately 13,000 T cells (gated on $CD3^+$ and on light-scatter parameters to exclude debris and aggregates).*

H3, and H4. Histone H1 associates with the linker DNA that interconnects neighboring nucleosomes and further condenses chromatin by interacting with histone proteins within the nucleosomal core.[21,22] Although apoptosis has been reported to result in marked morphological changes in chromatin organization, including condensation and eventual fragmentation of the nuclear DNA,[10,23,24] few data are available on the specific role of histones in this process. Here, using flow cytometric analysis of activated PBTs, we have found a striking correlation between immunodetection of histone H2B protein and apoptosis. Histone H2B immunoreactivity and DNA fragmentation were not detectable in freshly isolated PBTs, but upon activation with PMA plus ionomycin, phytohemagglutinin, or anti-CD3 antibody, these cells displayed a common pattern of double staining for histone H2B and DNA stand breaks. Indeed, kinetic analyses and the pattern of staining (ie, the ubiquitous presence of a small $H2B^+$/stand-break-negative population) strongly suggested that histone immunoreactivy develops during the early stages of activation-induced apoptosis, before the presence of detectable DNA strand breaks. Western blot analysis and confocal fluorescence microscopy of apoptotic and viable cells provided additional evidence for an association between histone immunoreactivity and T cell apoptosis, with the latter technique also demonstrating that histone immunoreactivity typically corresponded to the area of condensed chromatin in apoptotic cells.

Taken together, these data strongly suggest that the detection of histone H2B protein occurs as a result of early changes in the chromatin structure of

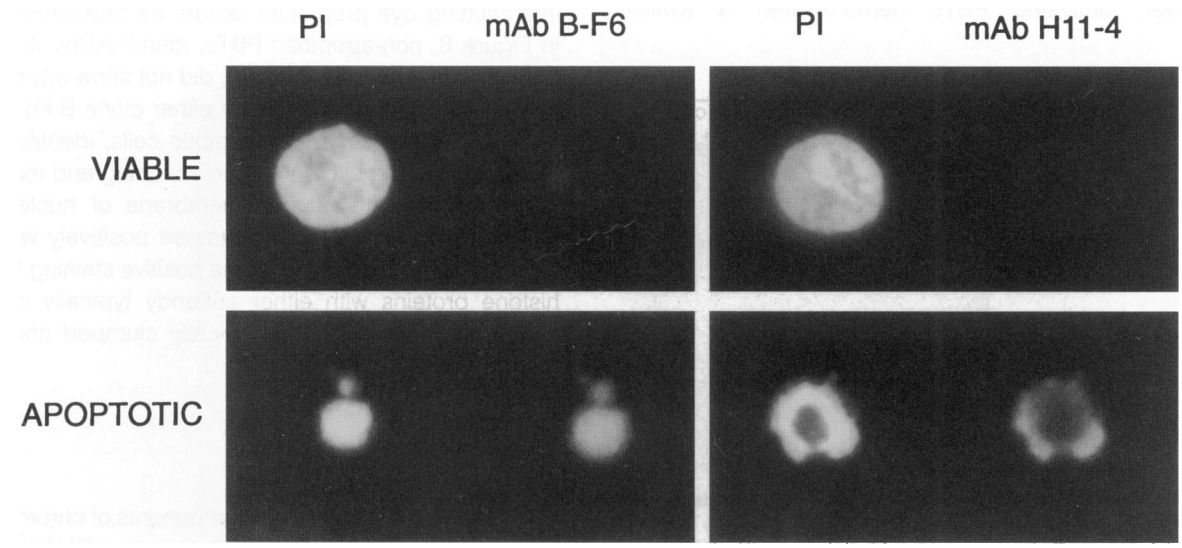

Figure 8. *Confocal microscopy indicates that detection of histone protein co-localizes with the condensed chromatin in apoptotic PBTs but is not detectable in normal non-apoptotic T cells with diffuse DNA. The 40-hour PMA plus ionomycin-activated PBTs were first stained with either MAb B-F6 or H11–4 followed by FITC-conjugated secondary antibody. Cells were then stained with propidium iodide in the presence of RNAse* A: *Representative dual-excitation images were collected on a Bio-Rad confocal microscope at a final magnification of ×2000. Cells stained with either an anti-histone MAb/FITC-second stage or propidium iodide alone showed no significant cross-over of fluorescence between the FITC and propidium iodide channels.*

apoptotic T cells before substantial cleavage of DNA and that these changes allow accessibility to otherwise hidden epitopes on the histone H2B protein. As we observed a correlation between apoptosis and the immunodetection of two distinct histone epitopes, we believe that our results are consistent with either a significant alteration in histone H2B structure and/or its relationship with adjacent histones, DNA, or other nuclear proteins. However, we cannot determine from our data alone whether the correlation between early apoptosis and histone immunoreactivity extends to all core histones or just histone H2B. The apoptosis-associated reactivity that we observed with the H11–4 pan-histone-reactive MAb may reflect either a specific change in H2B epitope display with the other histones remaining immunochemically silent or involvement of all core histones. Our results also suggest that these apoptosis-associated changes in histone immunoreactivity correlate with an increase in extractability of histone proteins by conventional (low ionic strength) lysis buffers. Laurent-Crawford et al[13] have also correlated the appearance of histones in total cellular extracts of HIV-infected T cells with apoptosis. In their study, all histone types were found to have increased extractability, suggesting that changes in chromatin structure during apoptosis may also include the non-H2B histones as well.

As mentioned above, our data suggest that histone immunoreactivity is an early event in apoptosis that precedes the oligonucleosomal DNA cleavage detected by the TDT reaction. We therefore believe that the apoptosis-associated change in histone epitope accessibility that we observed is not simply a by-product of a nonspecific opening of nucleosomal structure due to extensive DNA cleavage. It should be noted that recent data suggest that oligonucleosomal cleavage of DNA is a mid-to-late event in apoptosis and that the formation of high molecular weight fragments of approximately 700, 300, and 50 kbp correlates better with the early chromatin alterations visible in pre-apoptotic cells.[25,26] As the detection of these early DNA cuts by the TdT assay is uncertain, the temporal and functional relationship between high molecular weight DNA cleavage and changes in histone structure remain to be elucidated.

Western blot analysis of PBTs sorted into apoptotic and viable cell populations revealed a greater abundance of extractable histone H2B (p17) in the apoptotic cells. However, we also detected lesser amounts of extractable histone H2B in the lysates of the viable T cell population. The detection of histone H2B in these Hoechst 33342^{low}/7-AAD^{-} T cell lysates was consistent with our flow cytometric studies in which we observed that a small population of B-F6^{+}/DNA-strand-negative cells was invariably present. As the delineation of viable and early apoptotic cells by the Hoechst/7-AAD staining protocol[16] relies on a poorly characterized change in the cellular uptake of the Hoechst 33342 dyes, it is possible that the so-called viable cell populations defined by the Hoechst 33342^{low} phenotype actually contain early apoptotic cells that would have altered (antibody-accessible and low-salt-extractable) histone H2B.

The changes in chromatin organization that would allow increased MAb accessibility to histone H2B epitopes may be due to specific post-translational modifications and/or proteolytic cleavage of the histone proteins themselves. In this regard, an increased accessibility of the core nucleosomal histones H3, H4, and H2B to monoclonal and polyclonal anti-histone antibodies has been observed after poly(ADP-ribosyl)ation of histone H1 as well as other histone proteins.[27] Poly(ADP-ribosyl)ation of histone proteins is mediated by poly(ADP-ribose) polymerase and is induced by DNA damage as part of the DNA repair process.[22,28–30] This catalytic mechanism may be operative early in apoptosis as well, possibly accounting for our observation of histone neoepitope display early in this process. Interestingly, in a number of systems,[31–33] poly(ADP-ribose) polymerase activity has been shown to diminish during the apoptosis process (coincident with the appearance of nucleosomal DNA fragments[31]) due to proteolytic cleavage by interleukin-1β converting enzyme-like proteases, suggesting that the potential contribution by poly(ADP-ribose) polymerase to apoptosis-associated chromatin alterations are likely confined to early time points.

The role of proteases in apoptosis has been shown not only by the cleavage of poly(ADP-ribose) polymerase but also by cleavage of other nuclear proteins.[34,35] Although we did not detect specific cleavage of H2B by Western blot analysis, it is possible that limited proteolysis (below detectability by SDS-PAGE/Western blot) may play a role in the apoptosis-associated changes in histone epitope display identified in this report. In this regard, proteolytic removal of the amino-terminal domains of core histone proteins has been implicated in the condensation of chromatin during development.[36]

The results presented here clearly define the immunodectection of histone epitopes as an excellent early marker of apoptotic T cells. Coupling this immunodetection with multiparameter flow cytometry offers the opportunity to correlate changes in histone

epitope display not only with DNA strand breakage as shown here but also with any number of other MAb-defined or fluorescent-dye-defined changes in cell surface, intracytoplasmic, and/or intranuclear structures that may occur during apoptosis (excluding only detection of those events that require an intact, viable cell throughout the staining and acquisition protocol). Such analyses may provide new insights into changes in chromatin structure that occur in the cell undergoing apoptosis as well as define the temporal relationship of these changes with cytoplasmic and cell surface events. Moreover, the correlated analysis of histone reactivity and conventional T cell subset-defining markers (eg, CD4/CD8, CD45RA/RO, and CD27) by multiparameter flow cytometry will allow the subset-specific assessment of apoptosis in complex cellular preparations. The early onset of changes in histone epitope display during T cell apoptosis may be a particular advantage in such analyses as it clearly precedes the general degradation of immunofluorescent staining that accompanies later stages of apoptosis (or other forms of cell death). Such an approach, for example, may allow earlier detection of apoptosis in HIV-infected lymphocytes and aid in the precise determination of which T cell subsets are most susceptible to this process.

Acknowledgments

The authors thank Dr. Richard Scheuermann, Dr. Georg Fey, and Bonnie Darnell for their helpful comments during the course of this study, Dr. Herb Hagler for assistance with confocal microscopy, and Shar Waldrop and Zoran Zdraveski for technical assistance.

References

1. MacDonald HR, Less RK: Programmed cell death of autoreactive thymocytes. Nature 1990, 343:225–228
2. Akbar AN, Salmon M, Savill J, Janossy G: A possible role for *bcl-2* in regulating T cell memory: a 'balancing act' between cell death and survival. Immunol Today 1993, 14:526–532
3. Crispe IN: Fatal interactions: Fas-induced apoptosis of mature T cells. Immunity 1994, 1:347–349
4. Smith CA, Williams GT, Kingston R, Jenkinson EJ, Owen JJT: Antibodies to CD3/T-cell receptor complex induce death by apoptosis in immature T cells. Nature 1989, 337:181–185
5. Odaka C, Kizaki H, Tadakuma T: T cell receptor-mediated DNA fragmentation and cell death in T cell hybridomas. J Immunol 1990, 144:2096–2105
6. D'Adamio L, Awad KM, Reinherz EL: Thymic and peripheral apoptosis of antigen-specific T cells might cooperate in establishing self-tolerance. Eur J Immunol 1993, 23:747
7. Janssen O, Wesselborg S, Heckl-Ostreicher B, Bender A, Schondlemaier S, Pechhold K, Moldenhauer G, Kabelitz D: T cell receptor/CD3-signalling induces death by apoptosis in human T-cell receptor $\gamma\delta$-positive T cells. J Immunol 1991, 146:35
8. Webb S, Morris C, Sprent J: Extrathymic tolerance of mature T cells: clonal elimination as a consequence of immunity. Cell 1990, 63:1249–1262
9. Kawabe Y, Ochi A: Programmed cell death and extrathymic reduction of $V\beta8^+$ $CD4^+$ T cells in mice tolerant to *Staphylococcus aureus* enterotoxin B. Nature 1991, 349:245–249
10. Arends MJ, Morris RG, Wyllie AH: Apoptosis: the role of endonuclease. Am J Pathol 1990, 136:593–608
11. Wyllie AH, Kerr JFR, Currie AR: Cell death: the significance of apoptosis. Int Rev Cytol 1980, 68:251–264
12. Gorczyca W, Gong J, Darzynkiewicz Z: Detection of DNA strand breaks in individual apoptotic cell by the *in situ* terminal deoxynucleotidyl transferase and nick translation assays. Cancer Res 1993, 1951, 53:1945
13. Laurent-Crawford AG, Krust B, Muller S, Riviere Y, Rey-Cuille MA, Bechet J-M, Montagnier L, Hovanessian AG: The cytopathic effect of HIV is associated with apoptosis. Virology 1991, 185:829–839
14. Jung T, Schauer U, Heusser C, Neumann C, Rieger C: Detection of intracellular cytokines by flow cytometry. J Immunol Methods 1993, 159:197–207
15. Picker LJ, Singh MK, Zdraveski Z, Treer JR, Waldrop SL, Bergstresser PR, Maino VC: Direct demonstration of cytokine synthesis heterogeneity among human memory/effector T cells by flow cytometry. Blood 1995, 86:1408–1419
16. Schmid I, Uittenbogaart CH, Giorgi JV: Sensitive method for measuring apoptosis and cell surface phenotype in human thymocytes by flow cytometry. Cytometry 1994, 15:12–20
17. Harlow E, Lane D: Antibodies: A Laboratory Manual. Cold Spring Harbor, NY, Cold Spring Harbor Laboratory Press, 1988, pp 524–525
18. Rault-Leonardon M, Atkinson MAL, Slaughter CA, Moomaw CR, Srere PA: *Azotobacter vinelandii* citrate synthase. Biochemistry 1995, 34:257–263
19. Nicoletti I, Migliorati G, Pagliacci MC, Grignani F, Riccardi C: A rapid and simple method for measuring thymocyte apoptosis by propidium iodide staining and flow cytometry. J Immunol Methods 1991, 139:271–279
20. Van Holde KE: Chromatin. New York, Springer-Verlag, 1989
21. Boulikas T, Wiseman JM, Garrard WT: Points of contact between histone H1 and the histone octamer. Proc Natl Acad Sci USA 1980, 77:127–131
22. Boulikas T: Poly(ADP-ribosyl)ation, DNA strand breaks, chromatin, and cancer. Toxicol Lett 1993, 67:129–150
23. Kerr JFR, Wyllie AH, Currie AR: Apoptosis: a basic

biological phenomenon with wide-ranging implications in tissue kinetics. Br J Cancer 1972, 26:239–257
24. Wyllie AH, Morris RG, Smith AL, Dunlop D: Chromatin cleavage in apoptosis: association with condensed chromatin morphology and dependence on macronuclear synthesis. J Pathol 1984, 142:67–77
25. Brown DG, Sun X-M, Cohen GM: Dexamethasone-induced apoptosis involves cleavage of DNA to large fragments prior to internucleosomal fragmentation. J Biol Chem 1993, 268:3037–3039
26. Sun X-M, Cohen GM: Mg^{2+}-dependent cleavage of DNA into kilobase pair fragments is responsible for the initial degradation of DNA in apoptosis. J Biol Chem 1994, 269:14857–14860
27. Huletsky A, de Murcia G, Muller S, Hengartner M, Menard L, Lamarre D, Poirier GG: The effect of poly(ADP-ribosyl)ation on native and H1-depleted chromatin: a role of poly(ADP-ribosyl)ation on core nucleosome structure. J Biol Chem 1989, 264:8878–8886
28. Boulikas T: DNA strand breaks alter histone ADP-ribosylation. Proc Natl Acad Sci 1989, 86:3499–3503
29. Mathis G, Althaus FR: Periodic changes of chromatin organization associated with rearrangement of repair patches accompany DNA excision repair of mammalian cells. J Biol Chem 1986, 261:5758–5765
30. Realini CA, Althaus FR: Histone shuttling by poly(ADP-ribosyl)ation. J Biol Chem 1992, 267:18858–18865
31. Kaufmann SH, Desnoyers S, Ottaviano Y, Davidson NE, Poirier GG: Specific proteolytic cleavage of poly-(ADP-ribose) polymerase: an early marker of chemotherapy-induced apoptosis. Cancer Res 1993, 53: 3976–3985
32. Lazebnik YA, Kaufmann SH, Desnoyers S, Poirier GG, Earnshaw WC: Cleavage of poly(ADP-ribose) polymerase by a proteinase with properties ICE-like. Nature 1994, 371:346–347
33. Tewari M, Quan LT, O'Rourke K, Desnoyers S, Zeng Z, Beidler DR, Poirier GG, Salveson GS, Dixit VM: Yama/CPP32β, a mammalian homolog of CED-3, is a CrmA-inhibitable protease that cleaves the death substrate poly(ADP-ribose) polymerase. Cell 1995, 81:801–809
34. Kaufmann SH: Induction of endonucleolytic DNA cleavage in human acute myelogenous leukemia cells by etoposide, camptothecin, and other cytotoxic anticancer drugs: a cautionary note. Cancer Res 1989, 52:5870–5878
35. Casciola-Rosen LA, Miller DK, Anhalt GJ, Rosen A: Specific cleavage of the 70-kDa protein component of the U1 small nuclear ribonucleoprotein is a characteristic biochemical feature of apoptotic cell death. J Biol Chem 1994, 269:30757–30760
36. Lin R, Cook RG, Allis CD: Proteolytic removal of core histone amino termini and dephosphorylation of histone H1 correlate with the formation of condensed chromatin and transcriptional silencing during *Tetrahymena* macronuclear development. Genes Dev 1991, 5:1601–1610